

# Absolute frequency measurement of the lithium $D$ lines: Precise determination of isotope shifts and fine-structure intervals

Dipankar Das and Vasant Natarajan\*

*Department of Physics, Indian Institute of Science, Bangalore 560 012, India*

(Received 21 December 2006; revised manuscript received 4 April 2007; published 22 May 2007)

We use a Rb-stabilized ring-cavity resonator to measure the frequencies of the  $D$  lines in  $^{6,7}\text{Li}$ . Li spectroscopy is done by exciting a well-collimated atomic beam with a perpendicular diode laser beam and monitoring the resulting fluorescence. We obtain frequencies of 446 789 597.791(30) MHz and 446 800 132.006(25) MHz for the  $D_1$  line and 446 799 650.653(60) MHz and 446 810 184.005(33) MHz for the  $D_2$  line in the two isotopes. These values are consistent with earlier measurements, but represent an order-of-magnitude improvement in uncertainty. The measurements allow us to determine precisely the isotope shift in the  $D$  lines and the fine-structure interval in the  $2P$  state, which resolve several discrepancies among earlier measurements. The small negative isotope shift in the interval appears inconsistent with theoretical estimates.

DOI: [10.1103/PhysRevA.75.052508](https://doi.org/10.1103/PhysRevA.75.052508)

PACS number(s): 32.30.Jc, 42.62.Eh, 32.10.Fn

## I. INTRODUCTION

High-precision laser spectroscopy on the lithium isotopes is of fundamental interest, both experimentally and theoretically. This is because Li has a relatively simple three-electron structure, and first-principles atomic calculations can be tested by comparing calculated values of atomic properties against experimental determinations. Advanced theoretical techniques such as Hylleraas variational calculations combined with QED recoil corrections [1] yield precise theoretical estimates of transition frequencies, isotope shifts, and fine-structure intervals. In particular, comparison of theory with experimental measurements of the isotope shift of various transitions can be used to determine the change in nuclear charge radius [2,3], thus permitting tests of nuclear models [4]. For example, high-resolution spectroscopy on the  $2S_{1/2} \rightarrow 3S_{1/2}$  two-photon transition shows that the charge radius decreases monotonically from  $^6\text{Li}$  to  $^9\text{Li}$  and then increases for  $^{11}\text{Li}$ , indicating the influence of halo neutrons [2].

Li is the simplest alkali-metal atom, but spectroscopy on Li has been limited by two facts: (i) that hot lithium vapor is highly reactive and attacks most glasses, making it difficult to make vapor cells, and (ii) that the hyperfine levels in the  $D_2$  line are closely spaced and not resolved, making it difficult to determine the line center precisely. To overcome the first problem, most experiments are done with an atomic beam and use a perpendicular laser beam to minimize Doppler broadening. However, there is still a question of systematic Doppler shifts arising from any small misalignment from perpendicularity. The  $D$  lines in  $^{6,7}\text{Li}$  have been previously studied for their transition frequencies, isotope shifts, and fine-structure interval, using a variety of methods. These include level crossing [5,6], optical double resonance [7–9], Fourier transform [10], frequency-modulation spectroscopy [11], and electro-optic modulation [3,12]. However, there is considerable spread in the results from previous measurements. Some of these results also appear inconsistent with the latest theoretical calculations [1].

In this work, we measure the absolute frequencies of the  $D$  lines in  $^{6,7}\text{Li}$  with  $\sim 0.1$  parts per billion (ppb) precision. The frequencies are measured with our well-established technique of using a Rb-stabilized ring-cavity resonator [13,14]. Li spectroscopy is done by exciting a collimated atomic beam with a tunable diode laser. By directly locking the laser on a given transition and measuring its frequency offset from a cavity resonance, we avoid a variety of systematic errors that are possible when recording a full spectrum (for example, errors due to calibration uncertainties and nonlinearities of the laser scan). However, in the case of the partially resolved  $D_2$  line, we cannot be sure of the lock point, hence we do have to scan across the full line and use detailed line-shape modeling to determine the location of a particular transition. Even for these transitions, the offset frequency is determined in a manner that is independent of laser-scan calibration. Our results for the transition frequencies are consistent with earlier measurements but represent significant improvement in accuracy. For the  $D_1$  isotope shift and  $^6\text{Li}$  fine-structure interval, our precise results resolve the discrepancies among earlier measurements. The  $D_2$  isotope shift is consistent with two of the previous measurements, but disagrees with the most recent measurement [3]. Finally, the  $^7\text{Li}$  fine-structure interval differs significantly from all previous measurements, though it is somewhat close to one recent measurement [12].

## II. EXPERIMENTAL DETAILS

Lithium has two stable isotopes:  $^6\text{Li}$  with  $I=1$  and natural abundance of 7.5%, and  $^7\text{Li}$  with  $I=3/2$  and natural abundance of 92.5%. The low-lying energy levels of the two isotopes are shown in Fig. 1. The natural linewidth of the  $D$  lines is 5.87 MHz [15]. Thus, the different hyperfine transitions in the  $D_1$  line ( $2S_{1/2} \rightarrow 2P_{1/2}$  transitions) are well separated and nonoverlapping, with four transitions in each isotope. However, for the  $D_2$  line ( $2S_{1/2} \rightarrow 2P_{3/2}$  transitions), the hyperfine levels in the excited state are too closely spaced to be resolved completely. Each partially resolved peak involves two or three hyperfine levels of the excited state, depending on angular momentum selection rules.

---

\*Electronic address: [vasant@physics.iisc.ernet.in](mailto:vasant@physics.iisc.ernet.in); URL: [www.physics.iisc.ernet.in/~vasant](http://www.physics.iisc.ernet.in/~vasant)

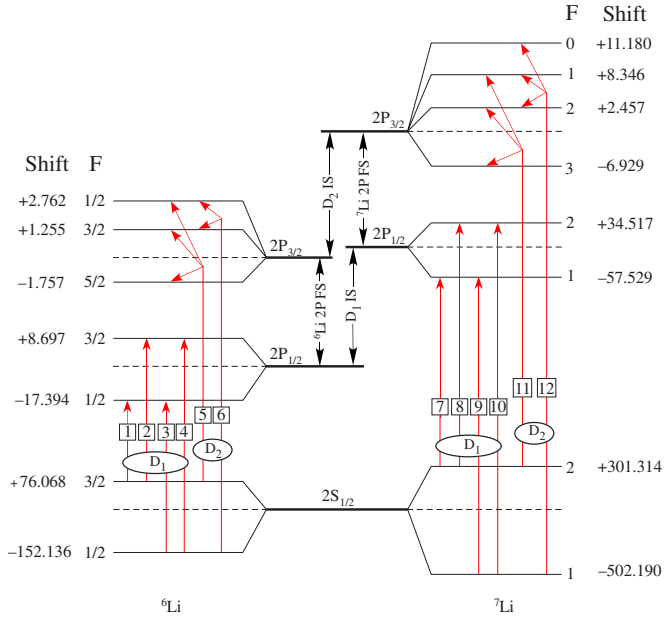


FIG. 1. (Color online) Relevant energy levels in  ${}^6,{}^7\text{Li}$ . Each hyperfine level is labeled with the value of its quantum number  $F$ , and the shift (in MHz) from the center of gravity of the state is given alongside. The various transitions from 1 to 12. Transitions in the  $D_2$  line are not fully resolved and are shown with the multiple hyperfine levels that couple to a given ground level. The tip of the vertical line indicates the approximate location of the peak center.

The frequency measurement technique has been described in detail in previous publications [13,16] and is just reviewed here briefly. As shown schematically in Fig. 2, we use a reference laser locked to one of the hyperfine transitions in the  $D_2$  line of  ${}^{87}\text{Rb}$  at 780 nm. The frequency of this transition is known with 6 kHz accuracy [17]. An evacuated ring-cavity resonator is locked to the reference laser, thereby fixing its length. The unknown laser is coupled into the locked cavity after shifting its frequency using an acousto-optic modulator (AOM). The AOM shift is locked in a feedback loop so that the cavity is in simultaneous resonance with both the reference laser and the shifted unknown laser. Thus a knowledge of the cavity length and the AOM offset gives the unknown frequency. For example, at some cavity length  $L$ , this length matches the resonance condition  $L=n\lambda$  with a mode number of  $n_{\text{ref}}=289\,810$  for the reference laser locked to the  $F=2 \rightarrow F'=(2,3)$  transition (frequency of 384 227 981.877 MHz [17]). The same length also matches the resonance condition for the unknown laser with a mode number of  $n_{\text{unk}}=336\,998$  when the laser frequency is AOM downshifted by exactly 14.165 MHz from the  $F=3/2 \rightarrow F'=1/2$  transition of the  ${}^6\text{Li}$   $D_1$  line. Thus the unknown frequency of this transition is determined to be 446 789 504.193 MHz. The cavity free-spectral range (FSR) at this length is 1325.793 MHz. The next nearest mode satisfying the resonance condition has an FSR differing by 400 kHz, which is 20 times the uncertainty with which the FSR is known.

In earlier work, we have shown that this method can be used to determine the frequencies of optical transitions with

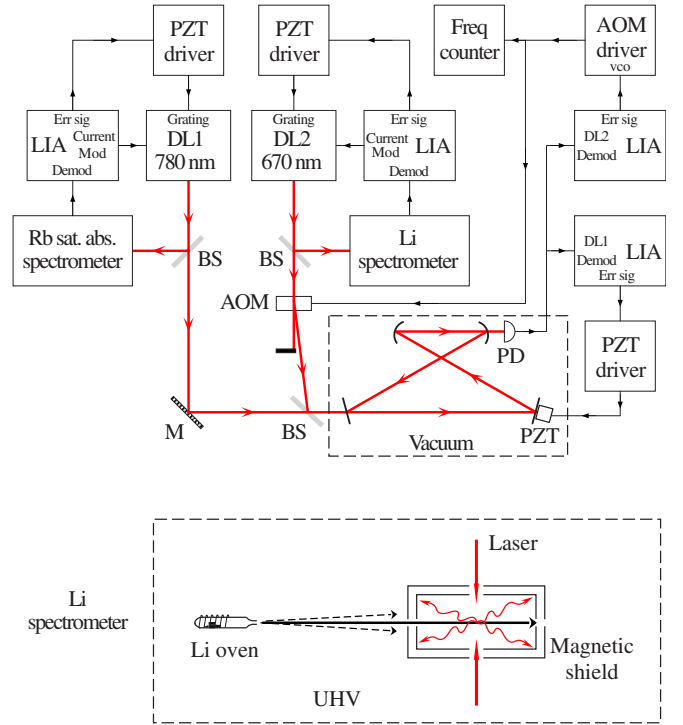


FIG. 2. (Color online) Schematic of the experiment. LIA: lock-in amplifier. DL: diode laser. PZT: piezoelectric transducer. AOM: acousto-optic modulator. BS: beam splitter. M: mirror. PD: photodiode. UHV: ultrahigh vacuum.

<0.1 ppb relative accuracy [13,14,16]. The linewidth of the cavity modes is about 35 MHz, and we can lock the AOM with about 10 kHz uncertainty. We have considered several sources of error, as listed in Table I. These errors depend on the atomic spectrometer, laser intensities compared to the saturation intensity, and stray magnetic fields. In particular, the effect of optical pumping into Zeeman sublevels can be a significant source of error. We minimize optical pumping effects by using linearly polarized light and reduce the splitting of magnetic sublevels by using a two-layer magnetic shield [18] around the interaction region, which reduces the stray field to below 5 mG (measured with a three-axis fluxgate magnetometer). In addition, there could be errors due to dispersion in the dielectric-coated cavity mirrors. We check for this by repeating the measurements at different cavity lengths [16].

TABLE I. Systematic errors in the measurement.

Source of error	Size (kHz)
Radiation pressure	10
Optical pumping into Zeeman sublevels	7–11
Laser lock to peak center	7
Differential phase shift at mirrors	15
Collisional shifts	<5
Misalignment into cavity (higher-order modes)	5

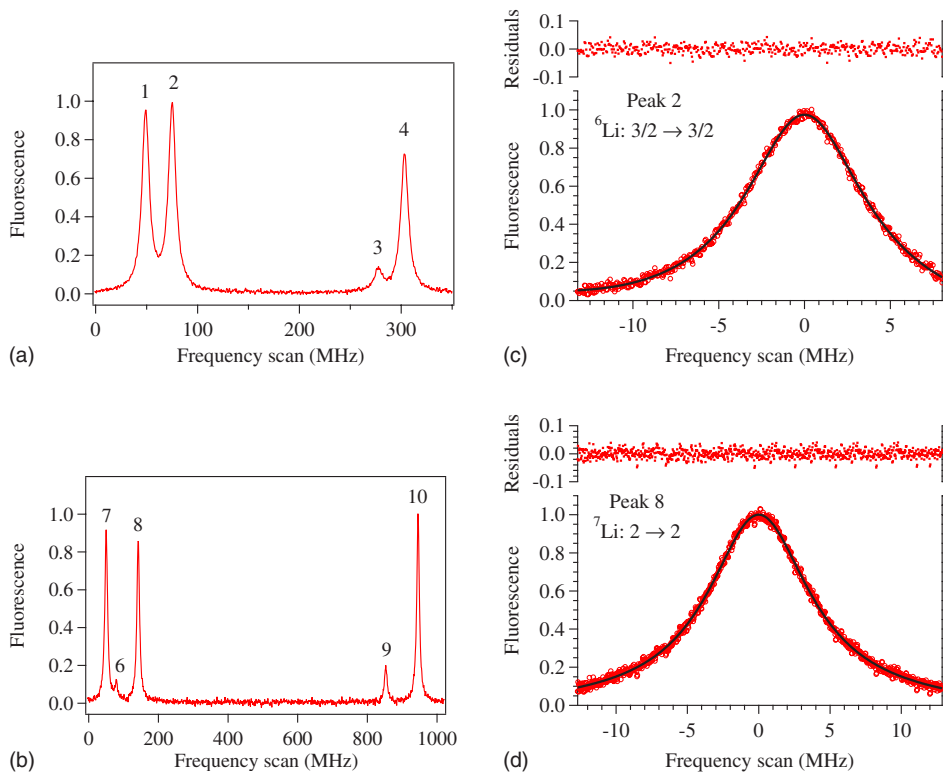


FIG. 3. (Color online)  $D_1$  line spectra in the two isotopes are shown in (a) and (b). The different hyperfine transitions are clearly resolved and are identified in Fig. 1. There is a large increase in the gain of the PMT for (a) compared to (b) to account for the low abundance of  ${}^6\text{Li}$ . In (c) and (d), we show close-ups of a representative transition in each isotope. The circles are the measured spectra, and the solid lines are Lorentzian fits. The fit residuals give an idea of the signal-to-noise ratio.

### A. Li spectroscopy

Li spectroscopy is done on a collimated atomic beam generated by heating a stainless steel oven containing Li metal to 300 °C. The oven is placed inside a vacuum chamber maintained at a pressure below  $5 \times 10^{-8}$  torr with a 20 l/s ion pump. The atomic beam is excited with a perpendicular laser beam generated from a homebuilt grating-stabilized diode laser system operating at 670 nm. The laser linewidth after feedback is less than 1 MHz. For locking, the laser is frequency modulated at  $f=20$  kHz and the fluorescence signal is demodulated at  $3f$  to generate the error signal. Such third-derivative locking minimizes peak-pulling errors. As mentioned before, optical pumping errors are reduced by using a linearly polarized laser beam and magnetically shielding the interaction region. The fluorescence signal is detected by a Hamamatsu R928 photomultiplier tube (PMT). Since the natural abundance of  ${}^6\text{Li}$  is very small, the gain of the PMT has to be increased substantially for spectroscopy on this isotope.

Li is a light atom, and the velocity from an oven at 300 °C is of the order of 1200 m/s. At these speeds, even a small misalignment angle from perpendicularity can cause a significant systematic Doppler shift. For example, a misalignment of 1 mrad causes a shift of 1.8 MHz in the transition frequency. We minimize this error by measuring the frequency with laser beams propagating from the left and right of the atomic beam. The Doppler shift will occur with opposite sign for the two counterpropagating beams and will cancel when we take the average. Indeed, their difference will give the size of the Doppler shift in each case. We check for parallelism of the counterpropagating laser beams by checking for beam overlap over a few meters and at the location of

an optical isolator placed in front of the diode laser.

Typical spectra for the  $D_1$  line in the two isotopes are shown in Figs. 3(a) and 3(b). The maximum laser intensity at the beam center is  $0.2 \text{ mW/cm}^2$ , compared to the saturation intensity of  $2.5 \text{ mW/cm}^2$ . The four hyperfine transitions in each isotope are clearly resolved. The peaks are labeled according to Fig. 1. Close-up scans (normalized) of peaks 2 and 8 are shown in Figs. 3(c) and 3(d), respectively. The solid lines are Lorentzian fits showing an excellent fit with featureless residuals. The size of the residuals gives an idea of the overall signal-to-noise ratio. As mentioned earlier, the gain of the PMT is much higher for (a) and (c). The fit linewidth is  $9.0 \pm 0.25 \text{ MHz}$  (compared to the natural linewidth of 5.87 MHz), which indicates that the atomic beam is well collimated because the spread in transverse velocity increases the total linewidth by only about 50%. The laser linewidth does not contribute significantly to this broadening.

Spectra from the  $D_2$  line are shown in Figs. 4(a) and 4(b). Each of the peaks represents multiple hyperfine transitions because of the close spacing of the levels. For  ${}^6\text{Li}$ , a close-up of peak 6 is shown in Fig. 4(c). The peak is obtained by locking the laser to peak 7 and using an AOM to scan across the nearby peak 6. Both the original laser beam and the AOM-shifted beam are mixed and sent across the atomic beam. Peak 6 is a convolution of two hyperfine transitions  $F=1/2 \rightarrow 3/2$  and  $F=1/2 \rightarrow 1/2$ . The solid curve is a two-peak Lorentzian fit with the spacing between the peaks kept fixed at the known hyperfine interval shown in Fig. 1. The relative amplitude between the two peaks is fixed at 0.8, which is the expected ratio from the Clebsch-Gordan coefficients for these two transitions. The fit linewidth for each transition is  $9.1 \pm 0.25 \text{ MHz}$ . The featureless residuals show

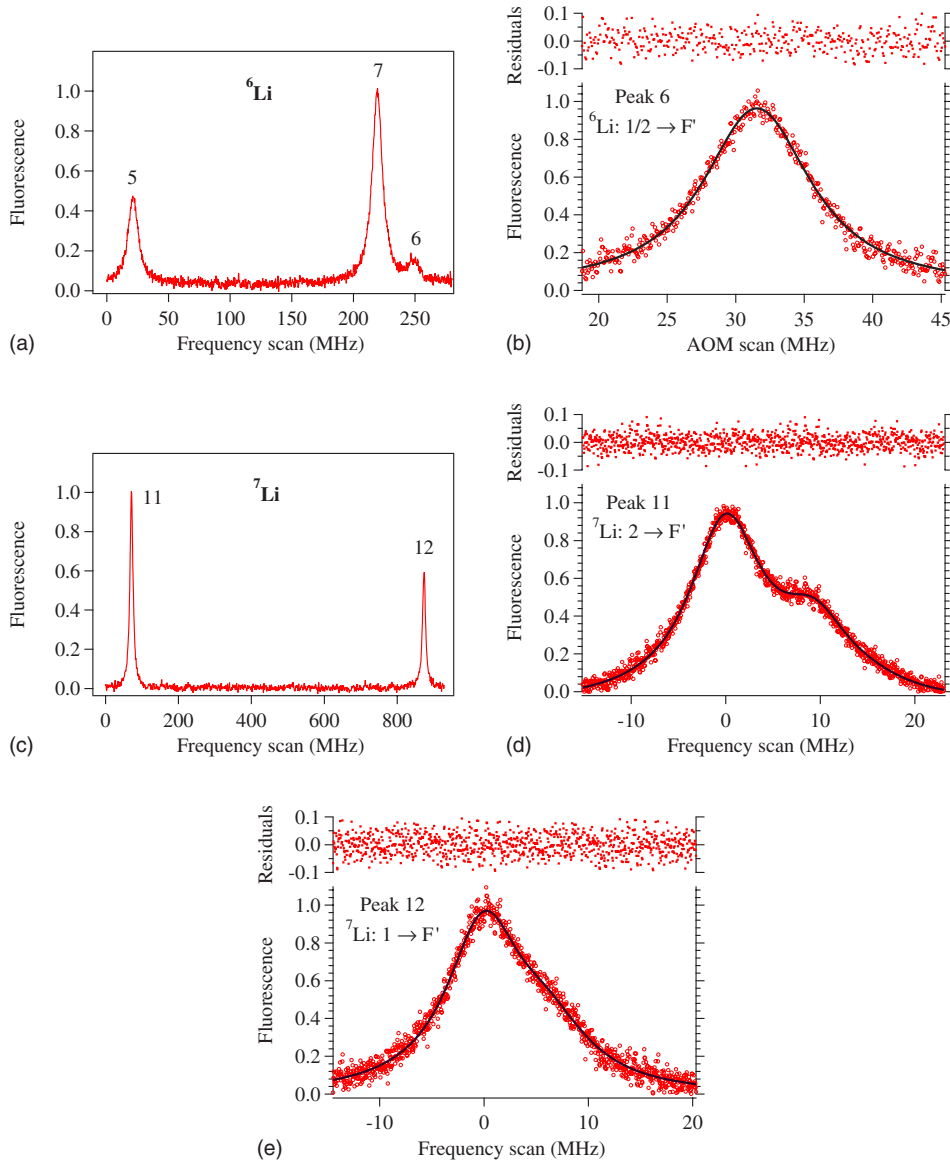


FIG. 4. (Color online)  $D_2$  line spectra in the two isotopes are shown in (a) and (b). The hyperfine levels in the excited state are closely spaced and only partially resolved. Close-ups of the three transitions used for the frequency measurements are shown in (c)–(e). The solid lines are multi-peak fits, as discussed in the text. The AOM offset in (c) is measured with respect to peak 7.

that the two-peak Lorentzian fits the data very well. This enables us to measure the exact AOM offset of the line center from peak 7.

In  $^7\text{Li}$ , the level spacing is slightly larger and the hyperfine transitions are partially resolved, as seen from the asymmetric line shapes in Figs. 4(d) and 4(e). For peak 11 shown in Fig. 4(d), the peak consists of three hyperfine transitions  $F=2 \rightarrow 3$ ,  $F=2 \rightarrow 2$ , and  $F=2 \rightarrow 1$ . The solid curve is a three-peak Lorentzian fit with their relative spacing fixed at 9.386 MHz and 5.889 MHz (from Fig. 1) and their relative intensities fixed according to the Clebsch-Gordan coefficients. The fit linewidth is  $9.4 \pm 0.25$  MHz. In this case, we have enough signal to noise to extract the hyperfine intervals from our spectra. If we leave the intervals as free fit parameters, then the average values from 22 spectra are 9.116(75) MHz and 6.099(100) MHz. This confirms that the three-peak model fits our spectra well and gives confidence in the location of the line center with respect to the observed line shape. For peak 12 shown in Fig. 4(e), the three hyperfine transitions  $F=1 \rightarrow 2$ ,  $F=1 \rightarrow 1$ , and  $F=1 \rightarrow 0$  are closer

with relative spacing of 5.889 MHz and 2.834 MHz. However, the three-peak Lorentzian again gives a good fit when the relative spacing and intensities are kept fixed. The fit linewidth is  $8.8 \pm 0.25$  MHz.

### III. RESULTS AND DISCUSSION

We first turn to the frequency measurements on the  $D_1$  line. Since the individual hyperfine transitions are well resolved, the laser could be locked to each peak and its frequency determined. Thus there are four measurements for each isotope, as listed in Table II. The measurements were repeated several times, and the final values listed have a statistical error of less than 10 kHz, or about 1 part in 1000 of the linewidth. To check for Doppler shift errors, the measurements were repeated with beams propagating from the left and right of the atomic beam, respectively. As can be seen, the difference between the two sets of data is about 300 kHz, which implies that the misalignment angle between the atomic and laser beam is only 0.09 mrad. Similarly, the

TABLE II. Measured frequencies for various hyperfine transitions on the  $D_1$  line for the two isotopes. The frequencies were measured at two cavity lengths  $L_1=226$  mm and  $L_2=178$  mm. In addition, the excitation laser beam propagated either from the right or the left of the atomic beam.

$D_1$ transition	Frequency at $L_1$ (MHz)		Frequency at $L_2$ (MHz)	
	Left	Right	Left	Right
${}^6\text{Li}: F=3/2 \rightarrow 1/2$	446 789 504.193	446 789 504.482	446 789 504.163	446 789 504.474
$F=3/2 \rightarrow 3/2$	446 789 530.215	446 789 530.577	446 789 530.247	446 789 530.515
$F=1/2 \rightarrow 1/2$	446 789 732.437	446 789 732.753	446 789 732.410	446 789 732.690
$F=1/2 \rightarrow 3/2$	446 789 758.491	446 789 758.785	446 789 758.449	446 789 758.755
${}^7\text{Li}: F=2 \rightarrow 1$	446 799 772.978	446 779 773.304	446 799 773.047	446 799 773.305
$F=2 \rightarrow 2$	446 799 865.024	446 779 865.376	446 799 865.087	446 799 865.389
$F=1 \rightarrow 1$	446 800 576.510	446 800 576.786	446 800 576.510	446 800 576.874
$F=1 \rightarrow 2$	446 800 668.541	446 800 668.849	446 800 668.563	446 800 668.881

measurements at cavity lengths of  $L_1=226$  mm and  $L_2=178$  mm are consistent within the stated uncertainty, indicating that dispersion at the mirrors is not a significant source of error at this level of precision.

### A. Consistency checks

There are two kinds of internal consistency checks that we do on the data, as listed below.

(i) The frequency of transitions to the same excited state from different ground states should differ by the ground-hyperfine interval. The ground-hyperfine interval is already known with extremely high accuracy through magnetic-resonance measurements [9], and this gives a stringent check on our measurements. As shown in Table III, there are four ways of obtaining this interval in each isotope. All the values lie within  $1\sigma$  of the known value.

(ii) The second check on the data is that the different hyperfine transitions should yield the same value for the hyperfine-free frequency of the line center. For the  $2P_{1/2}$  state, we have recently measured [19] the hyperfine constants to be  $A=17.394(4)$  MHz in  ${}^6\text{Li}$  and  $A=46.024(3)$  MHz in

${}^7\text{Li}$ . Since these are the most precise values of the constants, we use them in determining the line center. The center frequency in each case is determined by first taking the average from the right and left excitation beams, and then removing the shifts shown in Fig. 1. Thus there are eight independent values for each isotope, as listed in Table IV. These values are completely consistent with each other. This is illustrated by the fact that the standard deviation for the eight values is only 32 kHz in  ${}^6\text{Li}$  and 21 kHz in  ${}^7\text{Li}$ .

The average values of the center frequencies for the  $D_1$  line are

$${}^6\text{Li}, D_1: 446\,789\,597.791(30) \text{ MHz},$$

$${}^7\text{Li}, D_1: 446\,800\,132.006(25) \text{ MHz}.$$

The quoted error takes into account all the sources of systematic error listed in Table I. For example, the maximum error from optical pumping into Zeeman sublevels, assuming a worst case of complete optical pumping in a magnetic field of 5 mG, is 9.3 kHz for  ${}^6\text{Li}$  and 7.2 kHz for  ${}^7\text{Li}$ .

### B. Measurements on the $D_2$ line

As mentioned earlier, the various hyperfine transitions in the  $D_2$  line are very close to each other and are only partially

TABLE III. Consistency check 1. The frequency difference between transitions from the two ground levels to the same upper level ( $F'$ ) should match the known ground-hyperfine interval listed on the first line.

	Interval (MHz)
${}^6\text{Li}: \text{Ground hyperfine}$	228.205 261 1
$F'=1/2, \text{ at } L_1$	228.257
$F'=1/2, \text{ at } L_2$	228.232
$F'=3/2, \text{ at } L_1$	228.242
$F'=3/2, \text{ at } L_2$	228.221
${}^7\text{Li}: \text{Ground hyperfine}$	803.504 086 6
$F'=1, \text{ at } L_1$	803.507
$F'=1, \text{ at } L_2$	803.516
$F'=2, \text{ at } L_1$	803.495
$F'=2, \text{ at } L_2$	803.484

TABLE IV. Consistency check 2. The different transitions should yield the same value for the hyperfine-free frequency of the line center. The average value for the  $D_1$  line in  ${}^6\text{Li}$  is 446 789 597.791 MHz and in  ${}^7\text{Li}$  is 446 800 132.006 MHz.

$D_1$ transition	Center frequency (MHz)	
	$L_1$	$L_2$
${}^6\text{Li}: F=3/2 \rightarrow 1/2$	446 789 597.800	446 789 597.780
$F=3/2 \rightarrow 3/2$	446 789 597.767	446 789 597.752
$F=1/2 \rightarrow 3/2$	446 789 597.804	446 789 597.768
$F=1/2 \rightarrow 1/2$	446 789 597.852	446 789 597.807
${}^7\text{Li}: F=2 \rightarrow 1$	446 800 131.984	446 800 132.019
$F=2 \rightarrow 2$	446 800 131.997	446 800 132.034
$F=1 \rightarrow 2$	446 800 131.988	446 800 132.014
$F=1 \rightarrow 1$	446 800 131.987	446 800 132.031

resolved. Therefore, it is not possible to measure the frequency by locking the laser, since the exact lock point will not be precisely known. We have solved this problem in  ${}^6\text{Li}$  in the following manner. Since peak 6 in the  ${}^6\text{Li}$   $D_2$  line—i.e., the  $F=1/2 \rightarrow F'$  transitions—lies very close to peak 7 in the  ${}^7\text{Li}$   $D_1$  line, we can use an AOM to determine the small frequency difference between the two. To do this, the laser is first locked to peak 7. Then an AOM is used to generate a frequency-shifted beam, which is mixed with the original laser beam and sent across the atomic beam [20]. As the AOM is scanned, the fluorescence signal shows the line shape corresponding to peak 6. As discussed earlier, this line shape is fitted to a two-peak Lorentzian distribution to give the exact AOM offset for the  $F'=3/2$  level. The previously determined frequency of peak 7 is then added to determine the frequency of the  $F=1/2 \rightarrow 3/2$  transition. One advantage of this technique is that the offset frequency from peak 7 is (to first order) independent of any systematic Doppler shift since both peaks will shift equally. However, there will still be a differential shift due to the slightly different velocities of the two isotopes. Since the measurement was done with the same beam alignment as for the  $D_1$  line, the 15% difference in mass will cause a differential shift of 11 kHz. This is small compared to the total error of 60 kHz. Finally, the peak-pulling error due to peak 7 is also estimated to be much smaller than the total error since the separation is more than three linewidths.

For the  $D_2$  line of  ${}^7\text{Li}$ , this technique will not work because there are no nearby peaks to lock the laser to. Therefore, we use a slightly modified technique to determine the AOM offset to bring a transition into resonance for a given cavity length. We have used this technique earlier to determine the frequencies of unresolved peaks in Yb [21]. The basic idea is to scan the laser with a fixed AOM offset and simultaneously detect both the fluorescence and cavity transmission. Let us say we scan the laser across peak 11—i.e., the  $F=2 \rightarrow F'$  transitions—as shown in Fig. 5(a). The fluorescence line shape is fitted to a three-peak Lorentzian distribution as shown earlier in Fig. 4(d). This gives the exact location of the  $F'=3$  level relative to the cavity peak. However, the laser scan axis is not properly scaled and probably not completely linear. Therefore this procedure is repeated for different AOM offsets, chosen so that the cavity peak moves across the fluorescence peak. By fitting the separation as a function of AOM offset to a straight line [see Fig. 5(b)], we can determine the exact crossing point, and hence the exact AOM offset, that brings the  $F'=3$  level into resonance with the cavity. Note that the crossing point is independent of the scaling of the scan axis and depends only on how the separation varies with the AOM offset.

We have used this technique to determine the absolute frequencies of the  $F=2 \rightarrow 3$  transition (from peak 11) and the  $F=1 \rightarrow 2$  transition (from peak 12). The results for all measurements on the  $D_2$  line are shown in Table V. The total quoted error takes into account the various sources of error from Table I and additional uncertainty from the multipeak fit and knowledge of the hyperfine intervals. The center frequencies are determined by removing the shifts shown in Fig. 1. The two independent measurements in  ${}^7\text{Li}$  are consistent at the  $1\sigma$  level, even though the line shapes of the two

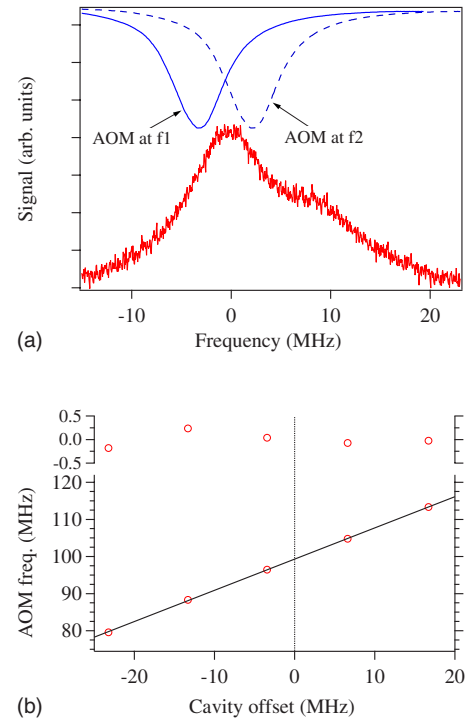


FIG. 5. (Color online) Measurement of the AOM offset for peak 11. In (a), the lower trace is the fluorescence signal, while the inverted peaks show the cavity resonance for two values of the AOM frequency. In (b), we plot the offset of the cavity resonance from the  $2 \rightarrow 3$  transition as a function of AOM frequency. The linear fit yields the zero-crossing point.

peaks used for these measurements are very different [see Figs. 4(d) and 4(e)]. The average values of the center frequencies for the  $D_2$  line are

$$\begin{aligned} {}^6\text{Li}, D_2: & 446\,799\,650.653(60) \text{ MHz}, \\ {}^7\text{Li}, D_2: & 446\,810\,184.005(33) \text{ MHz}. \end{aligned}$$

### C. Comparison to previous results

In Table VI, we compare our values for the transition frequencies to two previous measurements [11,22]. Our error is about an order of magnitude smaller than the values from the previous most-precise results in Ref. [11]. Our results are consistent with the values from this work at the  $1\sigma$  level (combined) for the  $D_1$  and  $D_2$  lines of  ${}^6\text{Li}$  and the  $D_2$  line of  ${}^7\text{Li}$ . Only for the  $D_1$  line of  ${}^7\text{Li}$  is our value higher by about  $3.5\sigma$ . However, our value for the isotope shift in this line, shown in Table VII, is consistent with recent measurements at the 100-kHz level [3,12]. Assuming that the value for the

TABLE V. Measurements on the  $D_2$  line.

$D_2$ transition	Frequency (MHz)	
	Transition	Center
${}^6\text{Li}: F=1/2 \rightarrow 3/2$	446 799 804.045(60)	446 799 650.653(60)
${}^7\text{Li}: F=2 \rightarrow 3$	446 809 875.637(40)	446 810 183.980(40)
${}^7\text{Li}: F=1 \rightarrow 2$	446 810 688.708(60)	446 810 184.061(60)

TABLE VI. Comparison of the absolute frequency of the  $D$  lines to published data.

Isotope	Line	Frequency (MHz)	Reference
${}^6\text{Li}$	$D_1$	446 789 597.791(30)	This work
		446 789 597.7(7)	[11]
		446 789 635(20)	[22]
	$D_2$	446 799 650.653(60)	This work
		446 799 650.5(5)	[11]
		446 799 685(20)	[22]
${}^7\text{Li}$	$D_1$	446 800 132.006(25)	This work
		446 800 130.6(4)	[11]
		446 800 163(20)	[22]
		446 800 117(117)	Theory [1]
	$D_2$	446 810 184.005(33)	This work
		446 810 183.8(4)	[11]
		446 810 205(20)	[22]
		446 810 170(117)	Theory [1]

$D_1$  frequency in  ${}^6\text{Li}$  is correct, the consistency of the  $D_1$  isotope shift becomes a check on the value of the  $D_1$  frequency in  ${}^7\text{Li}$ . Theoretical estimates of the transition frequencies in  ${}^7\text{Li}$  [1] are also shown in Table VI, but the calculations have a large uncertainty of 117 MHz.

As seen from the comparison of the  $D_1$  isotope shift to published data in Table VII, the three most-recent measurements show a variation of about 1 MHz, although the stated errors are less than 0.15 MHz. Our value is consistent with all the measurements except the low one from Ref. [22], which is from the same group that reported an earlier (consistent) value in Ref. [25]. This suggests that the more recent measurement from this group is incorrect. Our value also agrees very well with the recent theoretical calculation of Ref. [1], which takes into account QED recoil corrections of order  $(\mu/M)\alpha^5 mc^2$ , where  $m$  is the electron mass and  $M$  is the nuclear mass. Our measurement can be combined with the calculation to determine the difference in nuclear charge radii between  ${}^6\text{Li}$  and  ${}^7\text{Li}$  using the expression

TABLE VII. Comparison to published data for the  ${}^7\text{Li}$ - ${}^6\text{Li}$  isotope shift (IS) in the  $D_1$  and  $D_2$  lines. Units are MHz.

$D_1$ IS	$D_2$ IS	Reference
10 534.215(39)	10 533.352(68)	This work
10 534.039(70)	10 534.194(104)	[3]
10 534.26(13)	10 533.59(14)	[12]
10 533.13(15)	10 534.93(15)	[22]
10 532.9(6)	10 533.3(5)	[11]
10 534.3(3)	10 539.9(12)	[25]
10 534.13(7) $\pm$ 0.61 <sup>a</sup>	10 534.52(7) $\pm$ 0.61 <sup>a</sup>	Theory [1]

<sup>a</sup>Additional uncertainty due to the nuclear radii.TABLE VIII. Comparison to published data for the  $2P_{3/2}$ - $2P_{1/2}$  fine-structure splitting (FS) in the two isotopes and the  ${}^7\text{Li}$ - ${}^6\text{Li}$  splitting isotope shift (SIS). Units are MHz.

${}^6\text{Li}$ FS	${}^7\text{Li}$ FS	SIS	Reference
10 052.862(67)	10 051.999(41)	-0.863(79)	This work
10 052.964(50)	10 053.119(58)	0.155(60)	[3]
10 053.044(91)	10 052.37(11)	-0.67(14)	[12]
10 051.62(20)	10 053.4(2)	1.78(28)	[22]
10 052.76(22)	10 053.24(22)	0.48(31)	[5]
	10 053.184(58)		[8]
10 050.85(2) $\pm$ 3 <sup>a</sup>	10 051.24(2) $\pm$ 3 <sup>a</sup>	0.393(6)	Theory [1]

<sup>a</sup>Additional uncertainty due to mass-independent higher-order terms not yet calculated.

$$R_{\text{rms}}^2({}^7\text{Li}) - R_{\text{rms}}^2({}^6\text{Li}) = \frac{\text{IS}_{\text{meas}} - \text{IS}_0}{C}, \quad (1)$$

where  $\text{IS}_{\text{meas}}$  is the measured isotope shift,  $\text{IS}_0$  is the calculated shift without taking into account the shift due to the finite nuclear size [23], and  $C = -2.4565 \text{ MHz/fm}^2$  is a constant [1]. Thus our measurement gives a value of  $-0.83(3) \text{ fm}^2$  for the difference in nuclear radii, which overlaps with the recent result of  $-0.76(4) \text{ fm}^2$  also determined from the  $D_1$  isotope shift [3] and is much more accurate than the value of  $-0.79(25) \text{ fm}^2$  determined from nuclear scattering measurements [24].

For the isotope shift in the  $D_2$  line, there is again considerable spread among the previous measurements. In particular, the two recent values from the same group [3,12] and using the same technique differ by  $3.6\sigma$ , with stated errors below 140 kHz. Our value with an error of 68 kHz is consistent with their earlier measurement [12]. It is also consistent with the slightly less accurate value reported in Ref. [11]. Similar to the case of the  $D_1$  isotope shift, the two values from the same group in Refs. [25,22] differ significantly from each other (by about  $4\sigma$  here). These two values also disagree with all other measurements including ours. The large spread in experimental values gives an idea of the difficulty in measuring the  $D_2$  line. Furthermore, our value is about 1 MHz lower than the theoretical calculation, which is too large to be accounted for by the additional uncertainty of 0.61 MHz in the calculation due to the nuclear radius.

We now turn to a comparison of the  $2P_{3/2}$ - $2P_{1/2}$  fine-structure splitting (FS) in the two isotopes, as listed in Table VIII. In  ${}^6\text{Li}$ , the experimental values are all consistent with our value of 10 052.862(67) MHz within about  $1\sigma$ , except for the low value in Ref. [22], which is off by nearly  $6\sigma$ . Note that this is the same work where the  $D_1$  isotope shift was off by  $7\sigma$ . The theoretical calculation is 2 MHz lower, but there is a large uncertainty of  $\pm 3$  MHz due to mass-independent higher-order terms that are not yet included in the calculation. In  ${}^7\text{Li}$ , our value of 10 051.999(41) MHz is more than 1 MHz lower than most other measurements. It is closest to the result from Ref. [12], but even in this case the discrepancy is around  $3\sigma$  (combined). As in the case of the  $D_2$  isotope shift, the more recent value from this group [3]

has changed significantly (by  $6\sigma$  here and  $3.6\sigma$  for the isotope shift) and is inconsistent with our result. In some of the other measurements, it is not clear how the line center was obtained from the unresolved  $D_2$  line. As seen in Fig. 4, we have done a detailed line-shape analysis of the fluorescence spectra to extract the location of each transition. The theoretical calculation for the FS in  ${}^7\text{Li}$  is again lower (by 0.8 MHz here), but has the additional  $\pm 3$  MHz uncertainty mentioned earlier.

We finally consider the isotope shift in the FS, called the splitting isotope shift (SIS). The SIS is just the difference between the  $D_1$  and  $D_2$  isotope shifts or the  ${}^6\text{Li}$  and  ${}^7\text{Li}$  FS. All the previous measurements show a positive value for the SIS, except for Ref. [12]. We too obtain a *negative* value,  $-0.863(70)$  MHz, consistent with the only other negative result in Ref. [12]. However, the theoretical estimate for the SIS is *positive*,  $0.393(6)$  MHz [1]. The theoretical result is considered extremely reliable and has such a high accuracy because many sources of uncertainty in the calculation of the isotope shifts or FS (as listed in Tables VII and VIII) are common to both isotopes and will cancel when taking the difference. Hence our result, which is 1.3 MHz lower, is a value that disagrees strongly with theory, by  $16\sigma$  (experiment) and  $209\sigma$  (theory).

We thus see that the experimental situation in Li is quite unsatisfactory. This is apparent from the deviation plots shown in Fig. 6, where we show the spread in experimental values for the isotope shift and FS. First of all, it seems clear that Ref. [22] contains anomalous results, and therefore this (as well as the earlier results from this group in Ref. [25] which was supposedly supplanted by Ref. [22]) should not be included in the overall averages. The vertical lines in the figure indicate the location of the weighted mean of the previous measurements excluding these discrepant values. If we now consider the other measurements, the situation for the  $D_1$  isotope shift and the  ${}^6\text{Li}$  FS appears satisfactory, with good agreement among the previous measurements and ours. However, the situation is opposite for the  $D_2$  isotope shift and the  ${}^7\text{Li}$  FS. In particular, the recent measurements in Ref. [3] have further complicated the issue. Before this publication, the two valid results for the  $D_2$  isotope shift [11,12] were around 10 533.5 MHz. Combined with a mean value of 10 534.1 MHz for the  $D_1$  isotope shift, this implied a negative value for the SIS of  $-0.6$  MHz. On the other hand, the experimental values for the  ${}^7\text{Li}$  FS were clustered around 10 053.2 MHz. Combined with the value of 10 052.9 MHz for the  ${}^6\text{Li}$  FS, this implied a positive value for the SIS of  $+0.3$  MHz. Thus the isotope shift measurements implied a negative SIS and the fine-structure measurements a positive SIS. Clearly both cannot be right. The earlier result in Ref. [12] showed that the  $D_2$  isotope shift and the negative SIS are correct, and the  ${}^7\text{Li}$  FS is off by  $\sim 1$  MHz. The latest result from this same group [3] reaches the opposite conclusion, that the  ${}^7\text{Li}$  FS and the positive SIS are correct, and the value for  $D_2$  isotope shift should be higher.

In summary, it appears that our results for the  $D_2$  isotope shift, the  ${}^7\text{Li}$  fine-structure interval, and the SIS will become consistent with the recent measurement in Ref. [3], and the positive theoretical estimate for the SIS, if the frequency of the  $D_2$  line in  ${}^7\text{Li}$  increases by 1 MHz. We have tried hard to

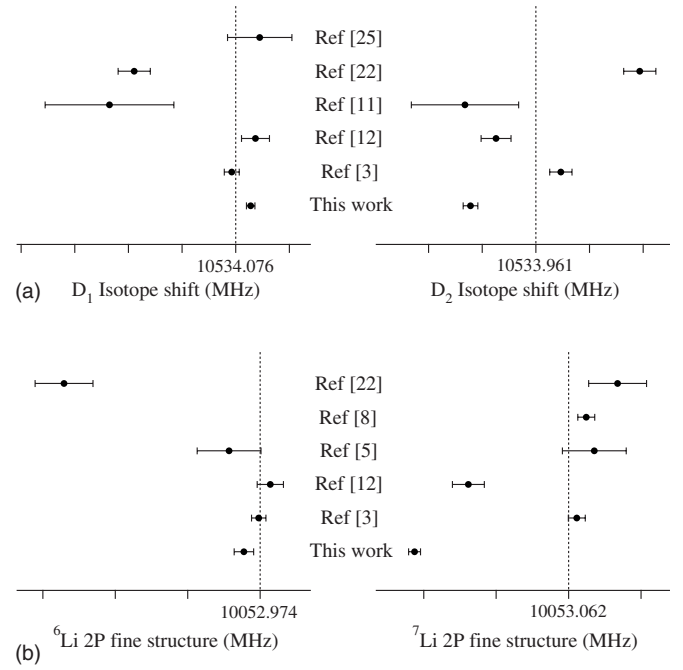


FIG. 6. Spread in experimental values. In (a), we show the measured values for the isotope shifts. The vertical line indicates the weighted mean of the previous measurements without including the anomalous results from Refs. [22,25], which are from the same group. The grid spacing is 0.5 MHz. In (b), we show a similar plot for measurements of the fine-structure interval, with the weighted mean again excluding the anomalous values from Ref. [22]. The two most recent results for  ${}^7\text{Li}$  from the same group (Refs. [3,12]) differ considerably.

look for systematic errors that would shift our value by this large amount, but without success. First of all, the shifted value would be inconsistent with the earlier measurement in Ref. [11]. Second, we have measured the  $D_2$  line in  ${}^7\text{Li}$  using both peaks 11 and 12, which have very different frequencies, line shapes, and hyperfine intervals. The consistency of these values suggests that our error estimate is reasonable. One potential source of error in atomic beam experiments is the Doppler shift due to misalignment of the laser beam from perpendicularity. However, we have seen from Table II that this shift is only about 150 kHz in our case. In addition, we have carefully shielded the interaction region from stray magnetic fields. On the other hand, it is not clear how some of the earlier experiments took care of the effects of Doppler shift, stray magnetic fields, and unresolved hyperfine levels in the excited state.

#### IV. CONCLUSION

In this work, we have measured the absolute frequencies of the  $D$  lines in  ${}^{6,7}\text{Li}$  with a tunable diode laser at 670 nm exciting a collimated atomic beam. The known frequency of a diode laser stabilized on the Rb  $D_2$  line at 780 nm is used as a frequency reference, and a ring-cavity is used to transfer it close to the unknown frequencies. We measure the frequencies with a relative precision of  $\sim 0.1$  ppb, which is about an order of magnitude better than previous measure-



ments. For the  $D_2$  line, the hyperfine levels are too closely spaced to be resolved completely. We use a multipeak fit of the observed line shape to extract the position of individual transitions.

We also obtain precise values for the isotope shift in the two lines, the fine-structure interval in the  $2P$  state, and the small isotope shift in the interval. There is a large spread among previous measurements of these quantities. Our value for the  $D_1$  isotope shift is consistent with recent measurements and the most-refined theoretical calculations. In addition, the difference in nuclear charge radius between  $^7\text{Li}$  and  $^6\text{Li}$  derived from our measurement is consistent with the value from nuclear scattering data, but is considerably more precise. The fine-structure interval in  $^6\text{Li}$  is also consistent with recent measurements and theoretical calculations. However, for the  $D_2$  isotope shift, while we agree with one previous high-precision measurement in Ref. [12], we disagree with a more recent measurement from the same group [3]

where they report a significantly higher value. For the  $^7\text{Li}$  fine-structure interval, our value is significantly lower than all the other values including the recent measurement in Ref. [3]. We are closest to the earlier value from this group [12]. Finally, we obtain a negative value for the splitting isotope shift, which was also obtained in Ref. [12], but appears completely inconsistent with theoretical calculations.

#### ACKNOWLEDGMENTS

We thank M. V. Suryanarayana for a critical reading of the manuscript. We are grateful to Wilhelm Kaenders of Toptica Photonics for supply of a wavelength-selected 670-nm laser diode. This work was supported by the Department of Science and Technology and the Board of Research in Nuclear Sciences (DAE), Government of India. One of us (D.D.) acknowledges financial support from the Council of Scientific and Industrial Research, India.

- 
- [1] Z. C. Yan and G. W. F. Drake, *Phys. Rev. A* **66**, 042504 (2002).
- [2] R. Sanchez *et al.*, *Phys. Rev. Lett.* **96**, 033002 (2006).
- [3] G. A. Noble, B. E. Schultz, H. Ming, and W. A. van Wijngaarden, *Phys. Rev. A* **74**, 012502 (2006).
- [4] S. C. Pieper, V. R. Pandharipande, R. B. Wiringa, and J. Carlson, *Phys. Rev. C* **64**, 014001 (2001).
- [5] K. C. Borg, T. G. Eck, and H. Wider, *Phys. Rev.* **153**, 91 (1967).
- [6] W. Nagourney, W. Happer, and A. Lurio, *Phys. Rev. A* **17**, 1394 (1978).
- [7] G. J. Ritter, *Can. J. Phys.* **43**, 770 (1965).
- [8] H. Orth, H. Ackermann, and E. W. Otten, *Z. Phys. A* **273**, 221 (1975).
- [9] E. Arimondo, M. Inguscio, and P. Violino, *Rev. Mod. Phys.* **49**, 31 (1977).
- [10] L. J. Radziemski, R. Engleman, and J. W. Brault, *Phys. Rev. A* **52**, 4462 (1995).
- [11] C. J. Sansonetti, B. Richou, R. Engleman, and L. J. Radziemski, *Phys. Rev. A* **52**, 2682 (1995).
- [12] J. Walls *et al.*, *Eur. Phys. J. D* **22**, 159 (2003).
- [13] A. Banerjee, D. Das, and V. Natarajan, *Opt. Lett.* **28**, 1579 (2003).
- [14] D. Das, S. Barthwal, A. Banerjee, and V. Natarajan, *Phys. Rev. A* **72**, 032506 (2005).
- [15] W. I. McAlexander, E. R. I. Abraham, and R. G. Hulet, *Phys. Rev. A* **54**, R5 (1996).
- [16] D. Das, A. Banerjee, S. Barthwal, and V. Natarajan, *Eur. Phys. J. D* **38**, 545 (2006).
- [17] J. Ye, S. Swartz, P. Jungner, and J. L. Hall, *Opt. Lett.* **21**, 1280 (1996).
- [18] Conetic AA Alloy, Magnetic Shield Corporation, Perfection Mica Co., Bensenville, Illinois, USA.
- [19] D. Das and V. Natarajan (unpublished).
- [20] Actually, the small frequency offset is generated by taking the difference of two AOMs, one with a fixed frequency and one whose frequency is scanned. The laser beam is double-passed through the scanning AOM to maintain directional stability. Further, its intensity is stabilized by feedback control of the rf power exciting the AOM.
- [21] A. Banerjee *et al.*, *Europhys. Lett.* **63**, 340 (2003).
- [22] W. Scherf, O. Khait, H. Jager, and L. Windholz, *Z. Phys. D: At., Mol. Clusters* **36**, 31 (1996).
- [23] For a slightly updated value of  $IS_0$ , see G. W. F. Drake, W. Nörtershäuser, and Z.-C. Yan, *Can. J. Phys.* **83**, 311 (2005).
- [24] C. W. de Jager, H. de Vries, and C. de Vries, *At. Data Nucl. Data Tables* **14**, 479 (1974).
- [25] L. Windholz, H. Jager, M. Musso, and G. Zezza, *Z. Phys. D: At., Mol. Clusters* **16**, 41 (1990).